Antiviral Research 134 (2016) 34–41

Contents lists available at ScienceDirect

Antiviral Research

journal homepage: www.elsevier.com/locate/antiviral

# *In vitro* inhibition of African swine fever virus-topoisomerase II disrupts viral replication

Ferdinando B. Freitas, Gonçalo Frouco, Carlos Martins, Alexandre Leitão, Fernando Ferreira*

*CIISA, Faculdade de Medicina Veterinária, Universidade de Lisboa, Av. da Universidade Técnica, 1300-477, Lisboa, Portugal*

ARTICLE INFO

*Article history:*
Received 8 April 2016
Received in revised form
23 August 2016
Accepted 24 August 2016
Available online 26 August 2016

*Keywords:*
ASFV-Topoisomerase II
qPCR
siRNA
Antiviral therapy
Vaccine development

ABSTRACT

African swine fever virus (ASFV) is the etiological agent of a highly-contagious and fatal disease of domestic pigs, leading to serious socio-economic impact in affected countries. To date, neither a vaccine nor a selective anti-viral drug are available for prevention or treatment of African swine fever (ASF), emphasizing the need for more detailed studies at the role of ASFV proteins involved in viral DNA replication and transcription. Notably, ASFV encodes for a functional type II topoisomerase (ASFV-Topo II) and we recently showed that several fluoroquinolones (bacterial DNA topoisomerase inhibitors) fully abrogate ASFV replication *in vitro*. Here, we report that ASFV-Topo II gene is actively transcribed throughout infection, with transcripts being detected as early as 2 hpi and reaching a maximum peak concentration around 16 hpi, when viral DNA synthesis, transcription and translation are more active. siRNA knockdown experiments showed that ASFV-Topo II plays a critical role in viral DNA replication and gene expression, with transfected cells presenting lower viral transcripts (up to 89% decrease) and reduced cytopathic effect (−66%) when compared to the control group. Further, a significant decrease in the number of both infected cells (75.5%) and viral factories per cell and in virus yields (up to 99.7%, 2.5 log) was found only in cells transfected with siRNA targeting ASFV-Topo II. We also demonstrate that a short exposure to enrofloxacin during the late phase of infection (from 15 to 1 hpi) induces fragmentation of viral genomes, whereas no viral genomes were detected when enrofloxacin was added from the early phase of infection (from 2 to 16 hpi), suggesting that fluoroquinolones are ASFV-Topo II poisons. Altogether, our results demonstrate that ASFV-Topo II enzyme has an essential role during viral genome replication and transcription, emphasizing the idea that this enzyme can be a potential target for drug and vaccine development against ASF.



## 1. Introduction

African swine fever (ASF) is a highly contagious hemorrhagic disease that affects domestic and wild suids. Clinical signs may vary from a hyperacute form, with 100% mortality, to a less common chronic and asymptomatic forms that can turn pigs into carrier state (Costard et al., 2009; Penrith and Vosloo, 2009). Until today there is no effective vaccine or treatment for ASF and control strategies include, among others, quarantine and compulsory slaughter of affected animals (reviewed in Gallardo et al., 2015; Michaud et al., 2013). The economic losses from these measures can disrupt both the local and, in severe outbreaks, the national economy due to international trade restrictions (Costard et al., 2009; Michaud et al., 2013). Nowadays, ASF is endemic in most of the sub-Saharan countries and in the Italian island of Sardinia for more than 35 years (Costard et al., 2009; Mur et al., 2016). In 2007, it was introduced in Georgia spreading to Armenia, Azerbaijan, Russia, to Ukraine in 2012 and, to Belarus in 2013 (reviewed in Sánchez-Vizcaíno et al., 2013, 2015). In 2014, ASF reached the European Union, namely Lithuania, Poland, Estonia and Latvia (reviewed in Sánchez-Vizcaíno et al., 2015). The etiological agent of the disease is the African swine fever virus (ASFV), a large (≈200 nm) enveloped icosahedral double-stranded DNA virus (170–190 kbp). ASFV is the only known *Asfarviridae* member and infects different species of soft ticks (*Ornithodoros* spp), wild and domestic pigs (reviewed in Boinas et al., 2014; Tulman et al., 2009). Its genome encodes for 151–167 genes depending on the strain,

* Corresponding author.
*E-mail address:* fernandof@fmv.ulisboa.pt (F. Ferreira).

http://dx.doi.org/10.1016/j.antiviral.2016.08.021
0166-3542/

however, about half of them lack any known or predictable function (Chapman et al., 2008; reviewed in Dixon et al., 2013). Remarkably, ASFV is the only known virus that infects mammals encoding for a protein with type II DNA topoisomerase activity (ASFV-Topo II) (Coelho et al., 2015), sharing high similarity with bacterial topoisomerases, although its sequence homology with eukaryotic type II topoisomerases is low (Baylis et al., 1992; García-Beato et al., 1992; Gadelle et al., 2003; Coelho et al., 2015). Type II topoisomerases control DNA topology during replication, transcription, chromosome condensation-decondensation and segregation by catalysing transient double-stranded breaks in one helix DNA, pass a second DNA helix, and then close the gate, in all forms of life (reviewed in Champoux, 2001; de Souza et al., 2010; Forterre et al., 2007).

Although previous studies show that several bacterial topoisomerase II inhibitors disrupt ASFV infection (Salas et al., 1983; Mottola et al., 2013), very little is known about the role of ASFV-Topo II during infection and how these drugs act. Indeed, more information about this protein, putatively involved in viral replication/transcription, is urgently needed to understand if ASFV-Topo II is a good target for drug development and/or vaccine design. In this study, qPCR was performed to investigate the transcription pattern of ASFV-Topo II gene during infection. siRNA technology was used to selectively knock down the ASFV-Topo II expression in order to analyze the role of this protein in viral replication and transcription, an approach that has been recently described to evaluate the importance of viral genes in West Nile virus infection (Anthony et al., 2009), Dengue virus (Wu et al., 2010; Ye et al., 2011), Influenza virus (Hirsch, 2010) and also in ASFV (Keita et al., 2010). Finally, a mechanism of action is proposed for the antiviral effects of fluoroquinolones, supported by the results obtained from the comet assay.

## 2. Material and methods

### 2.1. Cells and viruses

Vero cells from the European Collection of Cell Cultures (ECACC, Salisbury, UK) were maintained in DMEM (Dulbecco Modified Eagle's minimal essential medium) containing 10% (v/v) heat inactivated fetal calf serum, 1% of non-essential amino acids and Penicillin/Streptomycin at 100 units/ml and 100 μg/ml, respectively (all from Gibco, Life Technology, Karlsruhe, Germany). All experiments were conducted on actively replicating sub confluent cells grown at 37 °C under a 5% $CO_2$ humidified atmosphere (≥95%). The Vero-adapted ASFV strain (Badajoz, 1971, Ba71V) was used in all infections and propagated as previously described (Carrascosa et al., 2011). Viral suspension titrations were performed by observation of cytopathic effect (CPE) at end-point dilutions, using Vero cells inoculated with 10-fold serial dilutions of supernatants during 5 days and results were expressed as TCID50/ml (Spearman-Kärber endpoint method).

### 2.2. Cytopathic effect (CPE) evaluation

Cells were seeded, transfected and infected (MOI = 0.025 and 0.1) as described in siRNA delivery assay (see 2.8.). Using an inverted microscope, CPE's were evaluated by two researchers at 72 hpi, based on a four grade scale: 0 (no CPE), 33 (CPE ≤ 33%), 66 (CPE > 33% and ≤66%) and 100 (CPE > 66%), as previously described (Servan de Almeida et al., 2007; Keita et al., 2010). CPE values were calculated as the arithmetic mean of the two individual scores.

### 2.3. RNA extraction and cDNA synthesis

For all qPCR quantifications total RNA was extracted using the RNeasy Mini Kit (Qiagen, Courtaboeuf, France). Possible DNA contaminants in the RNA preparation were eliminated by treatment in column with DNAse I (Qiagen). RNA concentrations and purity were measured (OD value at 260 nm and A260/A280 coefficient) using a spectrophotometer (NanoDrop, 2000c, Thermo Fisher Scientific, Waltham, USA) and only RNA samples showing high purity (A260/A280 ratio between 1.8 and 2.0) were used. 200 ng of each total RNA sample was reverse transcribed (Transcriptor First Strand cDNA Synthesis Kit, Roche, Basel, Switzerland), according to the manufacturer's instructions. The obtained cDNA was diluted (1/20) in ultra-pure water and stored at −20 °C until further use.

### 2.4. Recombinant plasmids

The amplified fragments were cloned into a pGEM-Teasy Vector System II (Promega, Madison, USA), and the plasmids were used to transform DH5α competent cells. The vector plasmids were isolated from bacteria using the Roche High Pure Plasmid Isolation Kit (Roche Applied Science, Germany), according to the manufacturer's manual. To determine whether the cloned DNA fragments (ASFV-Topo II, VP32, VP72 and Cyclophilin A) were incorporated into isolated vectors, the inserts were amplified by PCR and their sequences were confirmed. Following this step, the concentration of each plasmid preparation was determined by spectrophotometric absorbance (NanoDrop, model 2000c). Their corresponding copy number was calculated using the equation: pmol (dsDNA) = μg (dsDNA) × 1515/DNA length in pb (pmol = picomoles, dsDNA = double-strand DNA, DNA length in pb = number of base pairs from the amplified fragment; 1 mol = 6022 × 1023 molecules).

### 2.5. Standard curves optimization

A ten-fold serial dilutions of each plasmid (ASFV-Topo II, VP32, VP72 and Cyclophilin A), ranging from $1 \times 10^{-1}$ to $1 \times 10^{-9}$ were initially used in duplicate to construct the standard curves in two different days. Threshold cycle (Ct) values obtained from each dilution were plotted against the logarithm of their initial template copy numbers and corresponding standard curves were generated by linear regression of the plotted points. From the slope of each standard curve, PCR amplification efficiency (E) was calculated according to the equation: E (%) = (10−1/slope−1)100% (Pfaffl, 2001).

### 2.6. Quantitative PCR

ASFV-Topo II, VP32, VP72 and Cyclophilin A mRNA levels were quantified by qPCR using Maxima SYBR Green PCR Master Mix (Thermo Fisher) according to the manufacturer's instructions [12.5 μl of master mix, 2.5 μl of forward and reverse primers (50 nM each), 5 μl of water and 2.5 μl of cDNA)]. All qPCR reactions were performed in Applied Biosystems 7300 Real Time PCR system (Thermo Fisher) with the following thermal profile: 10 min at 95 °C for initial denaturation; 40 cycles of 15 s at 95 °C and 60 s at 60 °C, followed by a final denaturation step of 5 s at 65 °C with a 20 °C/s ramp rate and subsequent heating of the samples to 95 °C with a ramp rate of 0.1 °C/s. Quantification of ASFV-Topo II, VP32, VP72 and Cyclophilin A mRNA levels were determined by the intersection between the fluorescence amplification curve and the threshold line. The crossing point values of each plasmid obtained from different known concentrations were plotted in a standard curve used to determine the copy number of each transcript. The

values were determined using the comparative threshold cycle method, which compares the expression of a target gene normalized to the reference gene (Cyclophilin A). The validation of the reference gene was confirmed using the ANOVA test. The specificity of the qPCR assays was confirmed by melting curve analyses. The sequences of all primers used in this study are shown in Table 1.

### 2.7. Quantification of ASFV-Topo II, VP32, VP72 mRNA levels

To quantify the ASFV-Topo II mRNA expression levels during infection, Vero cells ($5 \times 10^5$) were seeded onto 30 mm dishes and infected with a multiplicity of infection (MOI) of 1.5 (ASFV-Ba71V isolate). After 1 h of adsorption, the virus inoculum was removed, the cells were washed twice and fresh DMEM was added. Total RNA was extracted at indicated time points after infection (2, 4, 6, 8, 10, 12, 14, 16, and 20 hpi). The extraction protocol, cDNA synthesis and qPCR amplifications were performed as previous described (see 2.3. and 2.6). Three independent experiments were performed to verify the reliability of the results.

### 2.8. siRNA assays

Four double-stranded siRNAs (ON-TARGETplus, Thermo Fisher Scientific) targeting different sequence regions of the ASFV-Topo II transcript were designed (siDESIGN Center, Thermo Fisher Scientific), based on the full genome sequence of ASFV Ba71V isolate (GenBank/EMBL, accession number: ASU18466). One siRNA against the GAPDH gene (siRNA-GAPDH; Silencer™ GAPDH siRNA human control number 4605; Ambion/Thermo Fisher Scientific) was used as a control in all siRNA assays. The siRNA sequences used in the study are shown in Table 2. All siRNAs duplexes were diluted at different final concentrations (10, 50 and 100 nM) in serum-free Opti-MEM (Gibco, Life Technology, Karlsruhe, Germany) and using 8 μl HiPerfect Transfection reagent (Qiagen, Courtaboeuf, France). Mixtures were incubated at room temperature for 20 min to allow the formation of transfection complexes. Thereafter, 100 μl of the transfection solution was incubated with $2 \times 10^4$ Vero cells cultured in 500 μl of DMEM supplement with 10% FBS in a 24-well plate during 8 h. One hour before infection, the culture medium was removed and fresh medium was added to allow recovery of the cells. Next, cells were infected with ASFV Ba71V (MOI = 0.025 and 0.1), the viral inoculum was removed 1 h after and further incubated at 37 °C for 72 h. The viability of transfected cells was assessed every 8 h until 72 h by phase-contrast microscopy. The different siRNAs were used individually or in combination (50 + 50 nM) and their antiviral effects were evaluated by titrating viral progeny, quantifying the number of infected cells, the CPE and mRNA levels (ASFV-Topo II, VP32 and VP72). Due to economic and practical reasons only the two siRNAs duplexes (including combinations) that showed higher inhibitory results (CPE reduction) were used in further assays.

### 2.9. Immunofluorescence and microscopy analysis

Cells were seeded onto glass coverslips ($2 \times 10^4$), in 24-well plates, transfected with ASFV-Topo II siRNA_III + IV, and infected with ASFV Ba71V isolate (MOI = 1). At 12 hpi, cells were fixed in 3.7% paraformaldehyde and HPEM buffer [25 mM HEPES (4-(2-hydroxyethyl)-1-piperazineethanesulfonic acid), 60 mM PIPES (piperazine-N,N′-bis 2-ethanesulfonic acid), 10 mM EGTA (ethylene glycol tetraacetic acid), 1 mM MgCl2] for 15 min at room temperature and permeabilized in PBS/Tx-100 1% for 5 min. Following this step, cells were washed in PBS, blocked with PBS/BSA 1% for 30 min and incubated with an anti-ASFV conjugated FITC serum (1:50). A mounting medium with DAPI (4′,6-diamidino-2-phenylindole), was used (Vectashield, Vector Laboratories, Peterborough, UK). All incubations were performed in a dark humidified chamber to prevent fluorochrome fading. Immunofluorescence analysis was performed using an epifluorescence microscope (Leica DMR HC model, Wetzlar, Germany), data sets were acquired by Adobe Photoshop CS5 software (Adobe Systems, Inc., San Jose, USA) and images were subsequently processed using the ImageJ open source software (version 1.46r).

### 2.10. Quantification of ASFV-Topo II, VP32 and VP72 transcripts after the siRNA treatments

Vero cells ($2 \times 10^4$) were transfected with the most efficient siRNA during 8 h. At 1 h post-transfection, cells were infected with Ba71V (MOI = 1) and at 16 hpi total RNA was extracted. To ensure high RNA concentrations, the siRNA assays were performed in quadruplicated. The extraction protocol, cDNA synthesis and qPCR amplifications were performed as previous described (see 2.3. and 2.6). The qPCR assay was performed in triplicate to ensure the biological relevance of the results.

### 2.11. Comet assay

Comet assay was performed using the alkaline technique (Singh et al., 1988). In brief, Vero cells ($2 \times 10^5$) infected with Ba71V (MOI = 1) were exposed to enrofloxacin (100 μg/ml) from 0 to 12 hpi or from 15 to 16 hpi. In addition, infected and non-exposed, non-infected exposed and non-exposed to enrofloxacin were used as controls. At indicated time points, cells were gently washed twice in PBS, trypsinized and embedded in 60 μl of low-melting-point agarose (0.7%, Lonza, Rockland, USA) prewarmed at 37 °C. The mixture was immediately pipetted onto frosted microscope slides precoated with a layer of 1% normal melting point agarose diluted in PBS (Sigma, St. Louis, USA), and allowed to jellify (4 °C, 10 min). Slides were then immersed in an alkaline lysis solution (2.5 M NaCl, 100 mM EDTA, 10 mM Tris-HCl, 1% Triton X-100, pH 10), for 1 h at 4 °C. Before electrophoresis, slides were incubated with a fresh cold electrophoresis buffer (1 mM EDTA, 300 mM

**Table 1**
List of used primers.

| Target | Primer designation | Sequence (5′–3′) | Coordinates[a] | Orientation |
|---|---|---|---|---|
| ASFV-Topo II | TOPOFw | TTGCCGCTTGCTATTATGGA | 133242-133261 | Forward |
| ASFV-Topo II | TOPORev | CGGGCCCAAGTGGTGTAC | 133292-133309 | Reverse |
| Cyclophilin A | CycloFw1 | AGACAAGGTTCCAAAGACAGCAG | – | Forward |
| Cyclophilin A | CycloRev | AGACTGAGTGGTTGGATGGCA | – | Reverse |
| Cyclophilin A | CycloFw2 | TGCCATCCAACCACTCAGTCT | – | Forward |
| VP72 | VP72Fw | ACGGCGCCCTCTAAAGGT | 88273-88290 | Forward |
| VP72 | VP72Rev | CATGGTCAGCTTCAAACGTTTC | 88322-88343 | Reverse |
| VP32 | VP32Rev | TCTTTTGTGCAAGCATATACAGCTT | 108162-108186 | Forward |
| VP32 | VP32Fw | TGCACATCCTCCTTTGAAACAT | 108228-108249 | Reverse |

[a] Primer coordinates are relative to Ba71V sequence used as template for primer design.

**Table 2**
List of siRNA sequences used.

| Target | siRNA designation | Sequence (5′–3′) | Target coordinates[a] | Orientation |
|---|---|---|---|---|
| ASFV-Topo II | ASFV_TOPOII_I | CCUAAUAGCACGAUACAUAUU | 790–808 | Sense |
| ASFV-Topo II | ASFV_TOPOII_I | PUAUGUAUCGUGCUAUUAGGUU | 790–808 | Antisense |
| ASFV-Topo II | ASFV_TOPOII_II | CCAUUAAGGCCGAUGCAAAUU | 815–833 | Sense |
| ASFV-Topo II | ASFV_TOPOII_II | PUUUGCAUCGGCCUUAAUGGUU | 815–833 | Antisense |
| ASFV-Topo II | ASFV_TOPOII_III | GGGCGGAACCAGAGUACUAUU | 2492–2510 | Sense |
| ASFV-Topo II | ASFV_TOPOII_III | PUAGUACUCUGGUUCCGCCCUU | 2492–2510 | Antisense |
| ASFV-Topo II | ASFV_TOPOII_IV | GGGCCUACGUCGAUAAGAAUU | 2618–2636 | Sense |
| ASFV-Topo II | ASFV_TOPOII_IV | PUUCUUAUCGACGUAGGCCCUU | 2618–2636 | Antisense |

[a] siRNA coordinates according to the relative position in gene nucleotide sequence (start at position 1, ATG).

NaOH) during 10 min to allow unwinding of DNA. Electrophoresis was performed at 0.83 V/cm on ice for 20 min. After the electrophoresis, slides were washed in neutralization buffer (0.4 M Tris-HCl, pH 7.5) during 15 min. All steps described above were carried out in the absence of light to avoid DNA damage. For DNA staining, slides were incubated with a nucleic acid staining solution (RedSafe Nucleic Acid Staining Solution, 0.02 μl/ml, iNtRON Biotechnology, Gyeonggi-do, South Korea), and visualized in an epifluorescence microscope (Leica DM R HC model, Wetzlar, Germany). For each sample, 5 randomly selected microscopic fields were captured using Adobe Photoshop CS5 software (Adobe Systems, Inc., San Jose, USA) and DNA damage was evaluated by comparing the intensity of the comet tails between the experimental groups.

### 2.12. Effect of enrofloxacin on ASFV transcription

To evaluate the effect of enrofloxacin on ASFV transcription, Vero cells ($2 \times 10^5$) were seeded into a 24-well plate, incubated at 37 °C and infected with ASFV-Ba71V isolate (MOI of 1). After 1 h of adsorption, the virus inoculum was removed, the cells were gently washed and then exposed to enrofloxacin (100 μg/ml) during 6, 12 and 24 h followed by extraction of total RNA. The extraction protocol, cDNA synthesis and qPCR amplifications were performed as previous described (see 2.3. and 2.6). Results represent the mean value of three independent experiments performed in different days.

## 3. Results

### 3.1. ASFV-topoisomerase II gene is transcribed from the early phase of infection

Our results showed that ASFV-Topo II transcripts are detected as early as 2 hpi, gradually increasing throughout the infection and reaching a maximum peak at 16 hpi (Fig. 1). Additionally, ASFV-Topo II viral gene is less transcribed than the two viral structural genes used as controls (VP32 and VP72). In order to ensure that the normalized mRNA levels of different viral genes are comparable, only qPCR reactions with efficiency values ranged from 90 to 91% and showing $R^2$ values > 0.987 were considered.

### 3.2. siRNAs targeting ASFV-Topo II impairs viral infection

The inhibitory activity of four siRNA duplex targeting ASFV-Topo II mRNA was initially screened by visualizing the viral-induced cytopathic effect (CPE). When Vero cells were transfected individually with siRNA III or IV (100 nM) or in combination between them (50 + 50 nM) prior to infection (MOI = 0.025) the induced CPE was reduced in 66%, whereas when siRNA oligos were individually used at 10 and 50 nM, a decrease of 33% was found. No additional

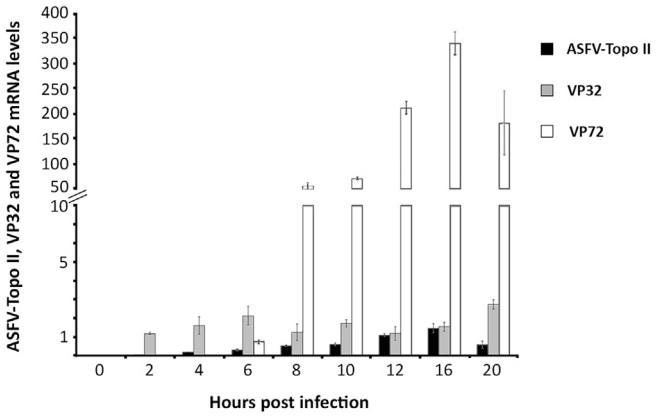


**Fig. 1. ASFV-Topo II is a late gene**. ASFV-Topo II transcripts were detected from 2 hpi onwards, reaching a maximum concentration at 16 hpi. Transcription levels were compared with VP32/VP72 mRNA levels and normalized to Cyclophilin A (reference gene). Error bars represent standard error of the mean from three independent experiences. (MOI of 1.5).

inhibitory effects were seen with increasing concentration beyond 100 nM (data not shown). In contrast, siRNA I or II did not showed any antiviral effects. As expected, the siRNA against GAPDH did not alter the viral CPE (Fig. 2a). Although similar results were observed when cells were infected with a MOI of 0.1, the reduction of CPE induced by ASFV was less obvious reaching a maximum value of 33% for the siRNA III or IV at 100 nM (data not shown). Considering the CPE inhibition observed in siRNA experiments, the supernatants harvested from the controls and from infected Vero cells transfected with siRNA III, IV (alone and combined) or siRNA GAPDH were used to infect new cells cultures, in order to assess the siRNAs effects on viral progeny. A virus titer reduction of 1.25–2.50 log was observed in infected cells transfected with siRNA III and IV (a decrease of 94.3–99.7%) in comparison with control groups (Fig. 2b).

Considering the role of type II topoisomerases in DNA synthesis and transcription and given our results, we assessed if siRNA III + IV against ASFV-Topo II had an effect in these processes by evaluating the number of infected cells and viral factories in Vero cells transfected with siRNA using immunofluorescence. Due to economical and practical reasons only this siRNA combination was used in this assay. A significant reduction (75.5%, $P < 0.002$) in the average number of infected cells was found between the group of transfected cells and the control group (7.30 ± 1.22, 29.80 ± 5.28, respectively), at 12 hpi (Fig. 3a and b). Regarding the number of ASFV factories per cell, a decrease was found in transfected cells when compared to control group (one factory: 5.30 ± 1.01, 19.50 ± 3.97, $P = 0.006$; two factories: 0.70 ± 0.33, 4.30 ± 0.94, $P = 0.004$ and three factories: 1.30 ± 0.42, 6.00 ± 1.25, $P = 0.005$), (Fig. 3c), with the number of each morphological type (circular or

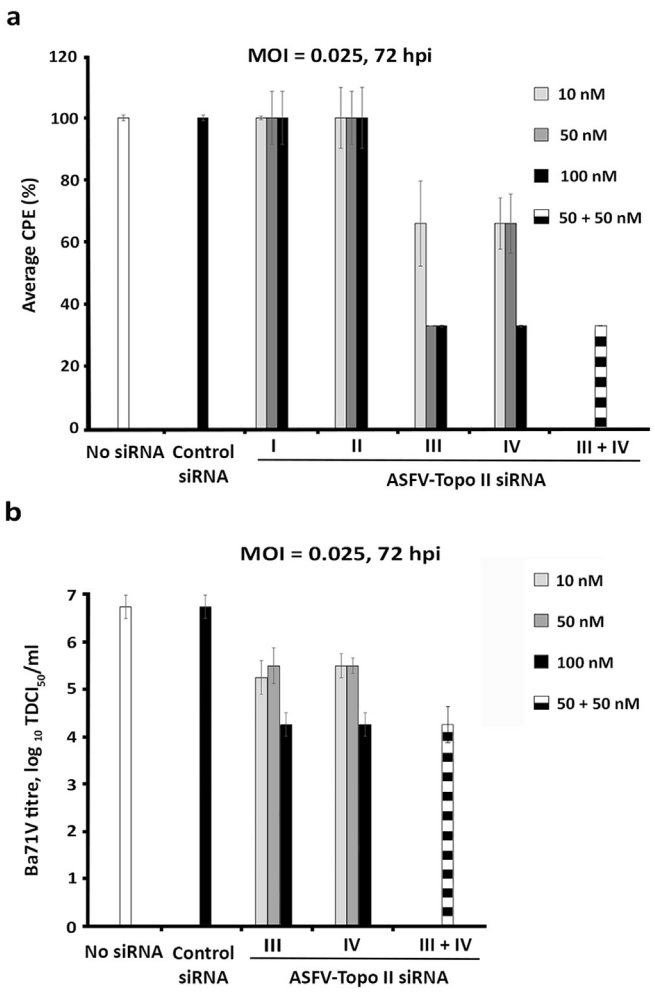


**Fig. 2. siRNAs against ASFV-Topo II inhibit ASFV replication**. a) A significant inhibition of CPE was observed when infected cells (MOI of 0.025) were transfected with siRNA_III or/and siRNA_IV. The CPE assay was performed as described previously (Keita et al., 2010). Error bars represent standard error of the mean from three independent experiences. (b) A reduction in virus yield was also found in infected cells transfected with siRNA_III and/or siRNA_IV (up to 99.9%). Error bars represent standard error of the mean from three independent experiences.

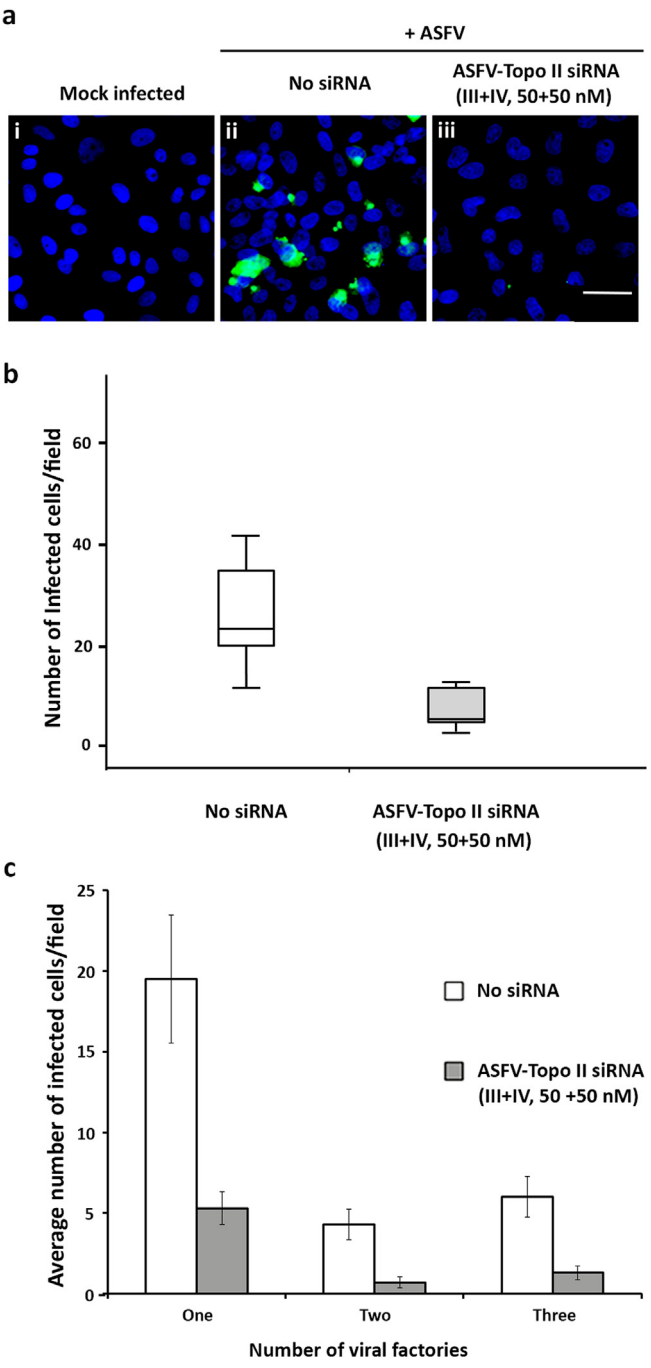


**Fig. 3. siRNAs anti-ASFV-Topo II inhibit the viral protein synthesis and the formation of viral factories sites**. A significant reduction in the number of infected cells was observed between the transfected group (siRNA_III + IV, 50 nM each) and the non-transfected group (Fig. 3a and b, P = 0.001). The average number of viral factories per cell was also lower in the transfected group than in control group (P = 0.002 for one factory and, P = 0.003 for two and three factories; Fig. 3c). Error bars represent standard error (±SE) of the mean of three independent experiments. Scale bar, 60 μm.

irregular) being significantly lower on transfected cells (circular *P = 0.010;* asymmetrical *P = 0.006*; data not shown). Although the above results suggest that ASFV-Topo II plays a key role during infection it remains to verify the efficiency of siRNA against the ASFV-Topo II mRNA and the impact in the viral transcription. For these propose, the mRNA levels of ASFV-Topo II and two viral structural genes were measured by qPCR. Results show a repression of the specific target transcript (up to 89%) but also a reduction in mRNA levels of VP32 (73%) and VP72 (77%) when compared with the infection control (Fig. 4).

### 3.3. Enrofloxacin acts as an ASFV-Topo II poison during infection

In previous studies it was shown that fluoroquinolones inhibit ASFV genome replication (Mottola et al., 2013), however the mechanism of action remains unknown, leading us to clarify the inhibitory effects of enrofloxacin during infection using a single cell electrophoresis analysis (comet assay). When ASFV-infected Vero cells were exposed to enrofloxacin from 15 to 16 hpi, a tail of fragmented DNA (comet) was observed (Fig. 5c), in contrast to infected cells exposed from the early phase of infection (0–12 hpi, Fig. 5f). As expected, no DNA fragmentation was identified in both infection control groups without any treatment (Fig. 5b and e) as in negative infection controls (Fig. 5a and d). Although, effects of enrofloxacin upon viral DNA were detected by comet assay, it remains to be verified whether this drug interferes with transcription. For this purpose, ASFV-Topo II, VP32 and VP72 mRNA levels were compared between the infection control and infected Vero cells exposed to enrofloxacin. In early phase of infection (6 hpi), no

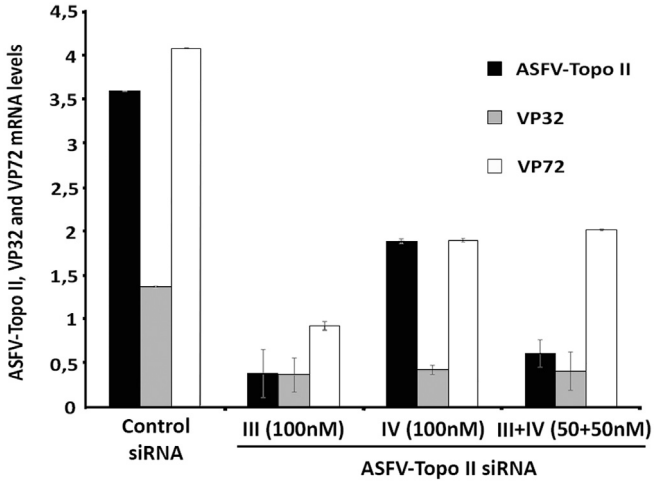


**Fig. 4. ASFV-Topo II siRNAs disrupt viral transcription**. The most effective siRNAs (III and IV) were able to reduce ASFV-Topo II mRNA levels up to 89%, VP32 mRNA levels up to 73% and VP72 gene transcription up to 77%. Transcripts levels were normalized to Cyclophilin A mRNA levels (reference gene) and error bars represent standard error of the mean from three independent experiences.

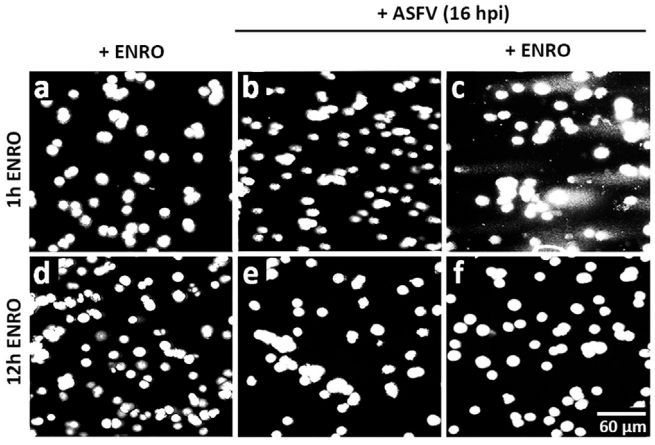


**Fig. 5. Enrofloxacin induces viral DNA breaks, thus acting as an ASFV-topoisomerase poison**. Although, the ASFV-infected Vero cells (MOI = 1) exposed to enrofloxacin from the early phase of infection (0–12 hpi) did not show viral DNA breaks or viral genomes (Fig. 5f), ASFV-infected Vero cells (MOI = 1) treated with enrofloxacin (100 µg/ml, 1 h) showed a tail of fragmented DNA (Fig. 5c). As expected, no DNA fragmentation was identified in both infected (Fig. 5b and e) and non-infected treated controls (Fig. 5a and d). Representative images of at least three independent experiments are shown. Scale bar, 60 µm.

changes were found in the viral transcript levels (ASFV-Topo II and VP32) between the non-exposed and exposed infected groups. At later times (12 and 24 hpi), ASFV-infected Vero cells exposed to enrofloxacin showed lower viral mRNA levels than control, while the transcript of the late gene VP72 was not detected at all (Fig. 6). This outcome strongly suggest that the fluoroquinolones are able to interfere with gene transcription by completely blocking the expression of later genes (e.g. VP72).

## 4. Discussion

Recently it was shown that ASFV encodes for a protein (ORF P1192R) that co-localizes with cytoplasmic viral factories at intermediate and late phases of infection, being able to complement a *Saccharomyces cerevisiae* Top2A temperature-sensitive mutant

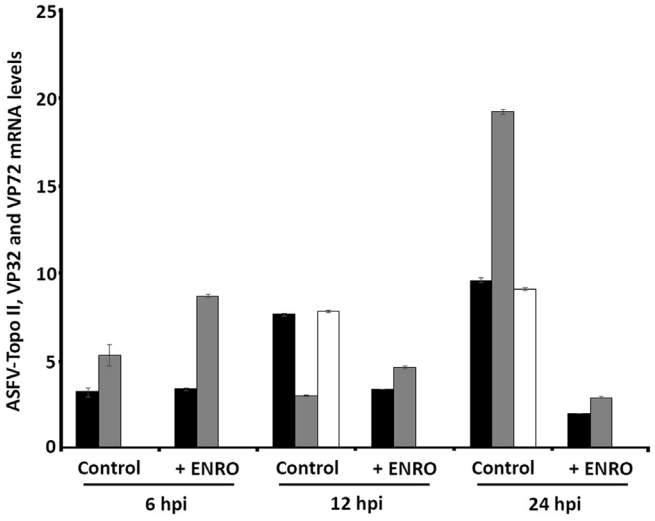


**Fig. 6. Enrofloxacin disrupts ASFV transcription activity**. Despite the fact that, at 6 hpi, ASFV-infected Vero cells (Ba71V, MOI = 1) exposed to enrofloxacin (100 µg/ml) showed similar ASFV-Topo II (black bars) and VP32 (grey bars) mRNA levels to infected control, at 12 hpi the mRNA levels of these genes become reduced and the transcripts of the late VP72 gene were not detectable (white bars). At 24 hpi, when a second infection cycle was already initiated, the ASFV-infected cells exposed to enrofloxacin showed a clear reduction in VP32 and ASFV-Topo II mRNA levels, in comparison to untreated cells, as the VP72 mRNA levels still absent. Transcripts levels were normalized to Cyclophilin A mRNA levels and error bars represent standard error of the mean from three independent experiences.

(Coelho et al., 2015). Although, phylogenetic studies revealed that ORF P1192R shares high sequence homology (Forterre et al., 2007) and functional motifs and domains with bacterial topoisomerases (Coelho et al., 2015), no further studies have been conducted to explore the role of ASFV-Topo II in ASFV infection. Using a well-established *in vitro* model of infection we showed that ASFV-Topo II mRNA levels continuously increase from 2 hpi to 16 hpi, similarly to other late ASFV genes (reviewed in Rodríguez and Salas, 2013). Most probably, the transcription kinetics of ASFV-Topo II indicates its need during the stage of accumulation of viral genomes that serve as templates for DNA replication and transcription, thus, showing an increasing number of topological complexities (e. g. knots, tangles and catenanes) that must be solved (reviewed in Rodríguez and Salas, 2013). Still, we cannot reject the possibility that ASFV-Topo II activity may also be required for other mechanisms like genome unpacking after virus entry or genome compaction before viral egress. Further, our siRNA experiments show that a partial depletion of transcripts encoding ASFV-Topo II reduces the viral-induced CPE, the ASFV progeny, the number of infected cells and also the number of viral factories per cell suggesting that viral transcription activity is diminished. Indeed, Vero cells transfected with siRNAs showed a reduction in mRNA levels of ASFV genes VP32 and VP72, early and late transcripts, respectively (Gil et al., 2008; Zhang et al., 2010). Even though viral transcription is repressed, we cannot exclude that depletion of ASFV-Topo II mRNA levels is in fact inhibiting viral DNA replication, avoiding the synthesis of an enough number of transcription templates to support viral progression. It is also important to refer that some of the siRNA did not induced a higher repression effect, though several siRNA combinations were used to prevent an eventual miss binding like described in other studies (Boden et al., 2003; Gitlin et al., 2005; Keita et al., 2010). In the present study enrofloxacin was found to induce ASFV DNA fragmentation when added at the intermediate-late phase of infection. This phase is characterized by a high rate of viral DNA replication (reviewed in Rodríguez and Salas, 2013) probably when ASFV-Topo II DNA

relaxation activity is more needed for viral genome segregation. In contrast, when ASFV-infected Vero cells are exposed to enrofloxacin from the early phase of infection, no viral genomes were detected suggesting that viral DNA synthesis was completely abolished. Although the mechanism of action of fluoroquinolones in bacteria is not fully understood, it is well known that these drugs target DNA gyrase and topoisomerase IV, blocking the replication machinery and inducing irreversible chromosome fragmentation (Drlica and Malik, 2003; Drlica et al., 2008; Malik et al., 2007). In a similar way, our results strongly suggest that enrofloxacin blocks the activity of ASFV-Topo II in infected cells, reinforcing previous *in vitro* studies (Mottola et al., 2013; Coelho et al., 2016), and further supporting that the mechanism of action is conserved between ASFV and bacteria. Probably, the enrofloxacin acts as a poison by trapping ASFV-Topo II on DNA and stabilizing cleavage complexes which leads to viral DNA fragmentation.

When infected cells were exposed to enrofloxacin from 2 hpi onwards, no VP72 transcripts were detected, whereas the early transcription of VP32 and ASFV-Topo II genes seems to be unaffected. These results corroborate a previous research in which enrofloxacin only disrupts late ASFV protein synthesis (Mottola et al., 2013). Overall our results suggest that ASFV-Topo II plays a major role in the intermediate-late phase of infection, probably by unwinding the viral DNA ahead of the transcription and replication machineries. Moreover it also unlikely that ASFV-Topo II is carried in the virion, since no changes in the transcription of early genes were found. Overall, our results strongly suggest that ASFV-Topo II plays a key role both at intermediate and late stages of viral infection, when viral DNA replication and transcription events are increased. However, we cannot exclude the possibility that this enzyme may also be involved in other early viral mechanisms (e.g unpacking of viral genomes, processing and control of genome concatemerization), since ASFV-Topo II transcripts were detected immediately after infection, reinforcing the idea that ASFV-Topo II could be a good candidate for the development of an effective vaccine or used as target for antiviral therapy.

## Conflicts of interests

The authors declared no potential conflicts of interest with respect to research, authorship, and/or publication of this article.

## Acknowledgments

This research was supported by the project grant (CIISA-UID/CVT/00276/2013), by the PhD fellowship from the Fundação para a Ciência e a Tecnologia (SFRH/BD/104261/2014), and by the European Union's Seventh Framework Programme (FP7/2007-2013) under grant agreement no 311931, ASFORCE.

## References

Anthony, K.G., Bai, F., Krishnan, M.N., Fikrig, E., Koski, R.A., 2009. Effective siRNA targeting of the 3' untranslated region of the West Nile virus genome. Antivir. Res. 82, 166–168. http://dx.doi.org/10.1016/j.antiviral.2008.12.007.

Baylis, S.A., Dixon, L.K., Vydelingum, S., Smith, G.L., 1992. African swine fever virus encodes a gene with extensive homology to type II DNA topoisomerases. J. Mol. Biol. 228, 1003–1010. http://dx.doi.org/10.1016/0022-2836(92)90887-P.

Boden, D., Pusch, O., Lee, F., Tucker, L., Ramratnam, B., 2003. Human immunodeficiency virus type 1 escape from RNA interference. J. Virol. 77, 11531–11535. http://dx.doi.org/10.1128/JVI.77.21.11531-11535.2003.

Boinas, F., Ribeiro, R., Madeira, S., Palma, M., de Carvalho, I.L., Nuncio, S., Wilson, A.J., 2014. The medical and veterinary role of Ornithodoros erraticus complex ticks (Acari: Ixodida) on the Iberian Peninsula. J. Vector Ecol. 39, 238–248. http://dx.doi.org/10.1111/jvec.12098.

Carrascosa, A.L., Bustos, M.J., de Leon, P., 2011. Methods for growing and titrating african swine fever virus: field and laboratory samples. Curr. Protoc. Cell Biol. 1–25. http://dx.doi.org/10.1002/0471143030.cb2614s53.

Champoux, J.J., 2001. DNA topoisomerases: structure, function, and mechanism. Annu. Rev. Biochem. 70, 369–413. http://dx.doi.org/10.1146/annurev.biochem.70.1.369.

Chapman, D.A.G., Tcherepanov, V., Upton, C., Dixon, L.K., 2008. Comparison of the genome sequences of non-pathogenic and pathogenic African swine fever virus isolates. J. Gen. Virol. 89, 397–408. http://dx.doi.org/10.1099/vir.0.83343-0.

Coelho, J., Ferreira, F., Martins, C., Leitão, A., 2016. Functional characterization and inhibition of the type II DNA topoisomerase coded by African swine fever virus. Virology 493, 209–216. http://dx.doi.org/10.1016/j.virol.2016.03.023.

Coelho, J., Martins, C., Ferreira, F., Leitão, A., 2015. African swine fever virus ORF P1192R codes for a functional type II DNA topoisomerase. Virology 474, 82–93. http://dx.doi.org/10.1016/j.virol.2014.10.034.

Costard, S., Wieland, B., de Glanville, W., Jori, F., Rowlands, R., Vosloo, W., Roger, F., Pfeiffer, D.U., Dixon, L.K., 2009. African swine fever: how can global spread be prevented? Philos. Trans. R. Soc. Lond. B. Biol. Sci. 364, 2683–2696.

de Souza, R.F., Iyer, L.M., Aravind, L., 2010. Diversity and evolution of chromatin proteins encoded by DNA viruses. Biochim. Biophys. Acta 1799, 302–318. http://dx.doi.org/10.1016/j.bbagrm.2009.10.006.

Dixon, L.K., Chapman, D.A.G., Netherton, C.L., Upton, C., 2013. African swine fever virus replication and genomics. Virus Res. 173, 3–14. http://dx.doi.org/10.1016/j.virusres.2012.10.020.

Drlica, K., Malik, M., 2003. Fluoroquinolones: action and resistance. Curr. Top. Med. Chem. 3, 249–282. http://dx.doi.org/10.2174/1568026033452537.

Drlica, K., Malik, M., Kerns, R.J., Zhao, X., 2008. Quinolone-mediated bacterial death. Antimicrob. Agents Chemother. 52, 385–392. http://dx.doi.org/10.1128/AAC.01617-06.

Forterre, P., Gribaldo, S., Gadelle, D., Serre, M.-C., 2007. Origin and evolution of DNA topoisomerases. Biochimie 89, 427–446. http://dx.doi.org/10.1016/j.biochi.2006.12.009.

Gadelle, D., Filée, J., Buhler, C., Forterre, P., 2003. Phylogenomics of type II DNA topoisomerases. Bioessays 25, 232–242. http://dx.doi.org/10.1002/bies.10245.

Gallardo, M.C., Reoyo, A., de la, T., Fernández-Pinero, J., Iglesias, I., Muñoz, M.J., Arias, M.L., 2015. African swine fever: a global view of the current challenge. Porc. Heal. Manag. 1, 1–14. http://dx.doi.org/10.1186/s40813-015-0013-y.

García-Beato, R., Salas, M.L., Viñuela, E., Salas, J., 1992. Role of the host cell nucleus in the replication of African swine fever virus DNA. Virology 188, 637–649. http://dx.doi.org/10.1016/0042-6822(92)90518-T.

Gil, S., Sepúlveda, N., Albina, E., Leitão, A., Martins, C., 2008. The low-virulent African swine fever virus (ASFV/NH/P68) induces enhanced expression and production of relevant regulatory cytokines (IFNalpha, TNFalpha and IL12p40) on porcine macrophages in comparison to the highly virulent ASFV/L60. Arch. Virol. 153, 1845–1854. http://dx.doi.org/10.1007/s00705-008-0196-5.

Gitlin, L., Stone, J.K., Andino, R., 2005. Poliovirus escape from RNA interference: short interfering RNA-target recognition and implications for therapeutic approaches. J. Virol. 79, 1027–1035. http://dx.doi.org/10.1128/JVI.79.2.1027-1035.2005.

Hirsch, A.J., 2010. The use of RNAi-based screens to identify host proteins involved in viral replication. Future Microbiol. 5, 303–311. http://dx.doi.org/10.2217/fmb.09.121.

Keita, D., Heath, L., Albina, E., 2010. Control of African swine fever virus replication by small interfering RNA targeting the A151R and VP72 genes. Antivir. Ther. 15, 727–736.

Malik, M., Hussain, S., Drlica, K., 2007. Effect of anaerobic growth on quinolone lethality with Escherichia coli. Antimicrob. Agents Chemother. 51, 28–34. http://dx.doi.org/10.1128/AAC.00739-06.

Michaud, V., Randriamparany, T., Albina, E., 2013. Comprehensive phylogenetic reconstructions of African swine fever virus: proposal for a new classification and molecular dating of the virus. PLoS One 8, e69662. http://dx.doi.org/10.1371/journal.pone.0069662.

Mottola, C., Freitas, F.B., Simões, M., Martins, C., Leitão, A., Ferreira, F., 2013. *In vitro* antiviral activity of fluoroquinolones against African swine fever virus. Vet. Microbiol. 165, 86–94. http://dx.doi.org/10.1016/j.vetmic.2013.01.018.

Mur, L., Iscaro, C., Cocco, M., Jurado, C., Rolesu, S., De Mia, G.M., Feliziani, F., Pérez-Sánchez, R., Oleaga, A., Sánchez-Vizcaíno, J.M., 2016. Serological surveillance and direct field searching reaffirm the absence of ornithodoros erraticus ticks role in african swine fever cycle in Sardinia. Transbound. Emerg. Dis. http://dx.doi.org/10.1111/tbed.12485 n/a–n/a.

Penrith, M.L., Vosloo, W., 2009. Review of African swine fever: transmission, spread and control. J. S. Afr. Vet. Assoc. 80, 58–62. http://dx.doi.org/10.4102/jsava.v80i2.172.

Pfaffl, M.W., 2001. A new mathematical model for relative quantification in real-time RT–PCR. Nucleic Acids Res. 29, e45. http://dx.doi.org/10.1093/nar/29.9.e45.

Rodríguez, J.M., Salas, M.L., 2013. African swine fever virus transcription. Virus Res. 173, 15–28. http://dx.doi.org/10.1016/j.virusres.2012.09.014.

Salas, M.L., Kuznar, J., Viñuela, E., 1983. Effect of rifamycin derivatives and coumermycin A1 on *in vitro* RNA synthesis by African swine fever virus. Brief report. Arch. Virol. 77, 77–80. http://dx.doi.org/10.1007/BF01314866.

Sánchez-Vizcaíno, J.M., Mur, L., Gomez-Villamandos, J.C., Carrasco, L., 2015. An update on the epidemiology and pathology of african swine fever. J. Comp. Pathol. 152, 9–21. http://dx.doi.org/10.1016/j.jcpa.2014.09.003.

Sánchez-Vizcaíno, J.M., Mur, L., Martínez-López, B., 2013. African swine fever (ASF): five years around Europe. Vet. Microbiol. 165, 45–50. http://dx.doi.org/10.1016/j.vetmic.2012.11.030.

Servan de Almeida, R., Keita, D., Libeau, G., Albina, E., 2007. Control of ruminant

morbillivirus replication by small interfering RNA. J. Gen. Virol. 88, 2307–2311. http://dx.doi.org/10.1099/vir.0.82981-0.
Singh, N., McCoy, M., Tice, R., Schneider, E., 1988. A simple technique for quantitation of low levels of DNA damage in individual cells. Exp. Cell Res. 175, 184–191. http://dx.doi.org/10.1016/0014-4827(88)90265-0.
Tulman, E.R., Delhon, G.A., Ku, B.K., Rock, D.L., 2009. African swine fever virus. Curr. Top. Microbiol. Immunol. 328, 43–87.
Wu, X., Hong, H., Yue, J., Wu, Y., Li, X., Jiang, L., Li, L., Li, Q., Gao, G., Yang, X., 2010. Inhibitory effect of small interfering RNA on dengue virus replication in mosquito cells. Virol. J. 7, 270.
Ye, C., Abraham, S., Wu, H., Shankar, P., Manjunath, N., 2011. Silencing early viral replication in macrophages and dendritic cells effectively suppresses flavivirus encephalitis. PLoS One 6, e17889.
Zhang, F., Moon, A., Childs, K., Goodbourn, S., Dixon, L.K., 2010. The African swine fever virus DP71L protein recruits the protein phosphatase 1 catalytic subunit to dephosphorylate eIF2alpha and inhibits CHOP induction but is dispensable for these activities during virus infection. J. Virol. 84, 10681–10689. http://dx.doi.org/10.1128/JVI.01027-10.